Multiple rotors-based photothermal agents for NIR-I/NIR-II fluorescence imaging-Guided tumor phototherapy

Naiwen Shi[1], Ruixin Zhang[1],Shankun Yao[1*], Qian Sun[1], Yanping Wu[1], Xiuzhi Yang[1], Ying Yang[1], Yehong Tan[4], Jingwen Zhang[4], Yuncong Chen[1,2,3*] and Zijian Guo[1,3*]

[1]State Key Laboratory of Coordination Chemistry, School of Chemistry and Chemical Engineering, Chemistry and Biomedicine Innovation Center (ChemBIC), ChemBioMed Interdisciplinary Research Center, Nanjing University, Nanjing 210023, China
[2]Department of Cardiothoracic Surgery, Nanjing Drum Tower Hospital, Medical School, Nanjing University, Nanjing 210008, China
[3]Nanchuang (Jiangsu) Institute of Chemistry and Health, Jiangsu, Nanjing 210000, China
[4]State Key Laboratory of Pharmaceutical Biotechnology, School of Life Sciences, Nanjing University, Nanjing 210023, China

*Corresponding authors: Yaosk@nju.edu.cn; chenyc@nju.edu.cn; zguo@nju.edu.cn;

1. Materials and instruments

Methods and materials Solvents were dried prior to use by a conventional method in organometallic chemistry. Commercially available chemicals were used as received. All air-sensitive compounds were reacted under the protection of the inert gases by using the Schlenk technique. Flash column chromatography (100-200 mesh) was carried out using silica gel purchased from Ding Kang Silica Gel Co. High resolution Mass spectra (HRMS) were recorded on an LCQ (ESI-MS, Thermo Finnigan) mass spectrometer. The 1HNMR and 13CNMR spectra were based on TMS, and the deuterated reagents were purchased from Plingweir. The ultrapure water for spectroscopic and cell culture was obtained from Millipore system (>18.2 MΩ). Morphology of nanoparticles were performed on transmission electron microscopy (TEM). The diameter of the nanoparticles was determined by dynamic light scattering (DLS) on an ELS-ZA2 (Otsuka Electronics Co., Ltd., Japan) with a semiconductor laser (50 nW) as a light source. Cell culture reagents such as cell culture medium DMEM and PBS buffer were purchased from Jiangsu KGI Biotech, and fetal bovine serum FBS and penicillin-streptomycin were purchased from Hyclone. Thiazole blue for MTT testing was purchased from Anage Chemical, and DMSO was purchased from Aladine. Confocal laser scanning microscope (CLSM) images were performed on Zeiss LSM710 confocal laser scanning microscope. An IVIS Lumina K Series III instrument (PerkinElmer) was used for optical imaging, and image analysis was realized with Living Image 4.5. Photothermal images were measured by NIR thermal imager (FLIR E40).

2. Synthesis

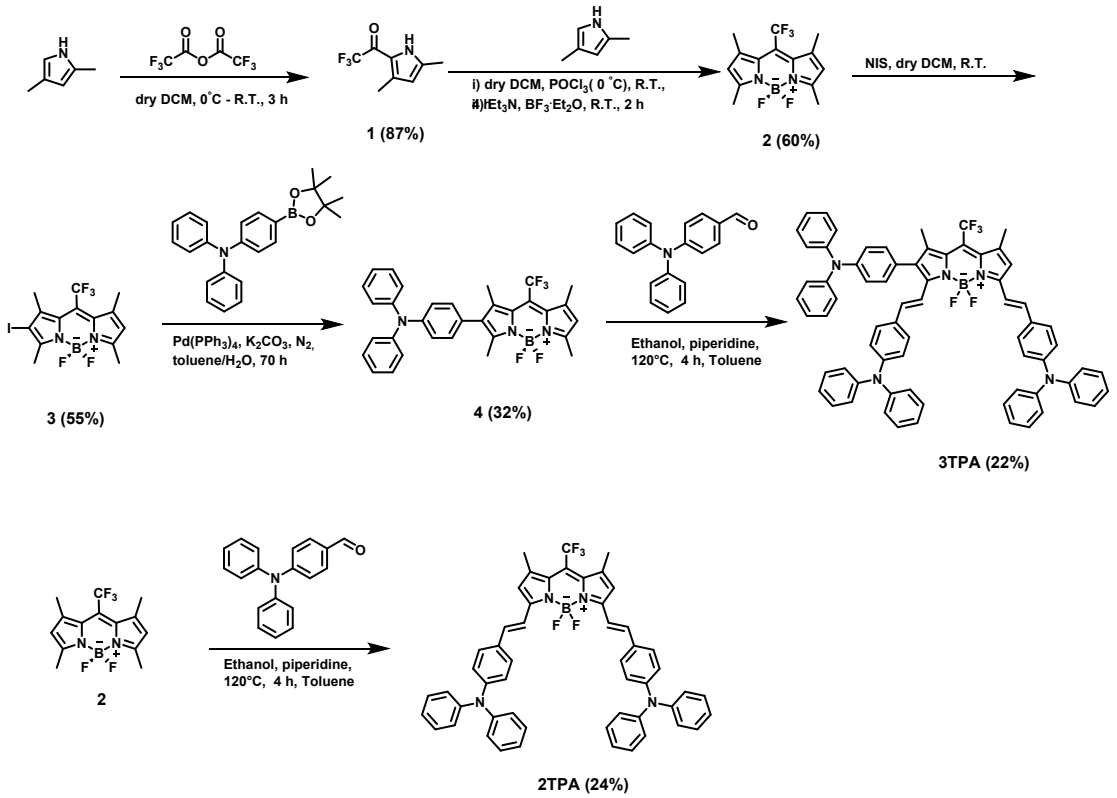

Scheme S1. Synthetic routes and chemical structures of **2TPA** and **3TPA**.

2.1 Synthetic of 1

To a stirred solution of 2,4-dimethylpyrrole (4.76 g, 50.0mmol) in dry dichloromethane (25 mL) at 0˚C was added trifluoroacetic anhydride (11.6 g, 55.0 mmol) under argon atmosphere. The resulting solution was stirred at 0˚C for 30 min, and warmed to room temperature. The reaction mixture was stirred at room temperature for 4 hours. Solvent was evaporated under reduced pressure and the crude product was purified on a silica-gel column using petroleum ether/ DCM mixture (1:4, v/v) as eluent to give the product as a white solid in 87% yield. ^{1}H NMR (400 MHz, $CDCl_3$) δ: 5.97 (d, J = 2.3 Hz, 1H), 2.34 (d, J = 19.3 Hz, 6H).

2.2 Synthetic of 2

To a stirred mixture of 2,4-dimethylpyrrole (0.746 g, 7.85 mmol) and compound **1** (1.00 g, 5.23 mmol) in dry dichloromethane (100 mL) at 0°C was added $POCl_3$ (1.04 g, 6.80 mmol) under argon atmosphere. The reaction mixture was warmed to room temperature and stirred for 4 h. This solution turned from colorless to red. The reaction mixture was added triethylamine (2.12 g, 20.1 mmol) and $BF_3{\cdot}OEt_2$ (4.45 g, 31.4 mmol) and stirred for 30 min. The combined organic layers were evaporated under reduced pressure. Solvent was evaporated under reduced pressure and the crude product was purified on a silica-gel column using petroleum ether/ DCM mixture (1:3, v/v) as eluent to give the product as a red solid in 60% yield. ^{1}H NMR (400 MHz, $CDCl_3$) δ: 6.15 (s, 2H), 2.54 (s, 6H), 2.30 (dd, J = 3.1, 6.3 Hz, 6H).

2.3 Synthetic of 3

2 (100 mg, 0.316 mmol) dissolved in 15 mL of dry dichloromethane. N-iodosuccinimide

(70.0 mg, 0.311 mmol) was added and stirred in the dark at room temperature for 12 hours. The mixture were extracted with sodium sulfate aqueous and CH_2Cl_2 three times, and the organic phases were combined and separated by column chromatography with CH_2Cl_2 as the eluent. The product was recrystallized from CH_2Cl_2/petroleum ether (1:5, v/v) as eluent to give the product as a blue solid in 55% yield. ^{1}H NMR (400 MHz, $CDCl_3$) δ: 6.22 (s, 1H), 2.63 (s, 3H), 2.55 (s, 3H), 2.31 (d, J = 3.0 Hz, 6H).

2.4 Synthetic of 4

Compound **3** (30.0 mg, 0.0679 mmol) and N,N-bis(4-methylphenyl)-4-(4,4,5,5-tetramethyl-1,3,2-dioxaborolan-2-yl)aniline (37.8 mg, 0.101 mmol) were dissolved in 5 mL of Toluene. Then, the aqueous solution of K_2CO_3 (48.9 mg in 1 mL of H_2O) was added, followed by adding 7.84 mg of $Pd(PPh_3)_4$. The mixture was refluxed at 90°C for 16 hours and cooled to room temperature. The crude mixture was then extracted by water and CH_2Cl_2, then dried by anhydrous $MgSO_4$ and the rotary evaporation. The crude product was obtained via column chromatography with CH_2Cl_2/petroleum ether (1:5, v/v) as eluent to afford compound **4** (11.5 mg, 30% yield). ^{1}H NMR (400 MHz, $CDCl_3$) δ: 7.29 (dd, J = 8.4, 7.5 Hz, 5H), 7.10 (ddd, J = 25.2, 10.2, 4.9 Hz, 10H), 2.54 (d, J = 8.7 Hz, 6H), 2.31 (d, J = 2.8 Hz, 3H), 2.21 (d, J = 3.2 Hz, 3H). ^{13}C NMR (400 MHz, $CDCl_3$) δ: 158.48, 147.62, 147.53, 142.75, 138.47, 136.55, 131.06, 129.52, 126.26, 124.98, 124.19, 123.97, 123.47, 122.75, 121.23, 77.48, 77.16, 76.84, 15.88, 15.80, 15.16, 14.67, 14.45.

2.5 Synthetic of 3TPA

A mixture of **4** (200 mg, 0.358 mmol) and 4-(diphenylamino)benzaldehyde (215 mg, 0.787 mmol) was dissolved in toluene, which was heated at 120 °C using acetic acid (0.08 mL) and piperidine (0.08 mL) as a catalyst. Then the mixture was poured into brine, extracted with CH_2Cl_2 three times (60 mL), then washed with brine and dried with anhydrous sodium sulfate. The solvent was removed by rotary evaporation, and the crude product was purified by column chromatography (silica gel, DCM : PE = 1 : 3.5, v/v) to afford compound **3TPA** (83.5 mg, 22% yield). ^{1}H NMR (400 MHz, CD_2Cl_2) δ: 7.60 (dd, J = 16.3, 6.9 Hz, 2H), 7.51 – 7.47 (m, 2H), 7.36 – 7.22 (m, 15H), 7.21 – 7.07 (m, 20H), 7.07 – 6.94 (m, 6H), 6.87 (s, 1H), 6.70 (d, J = 16.4 Hz, 1H), 2.38 (dd, J = 4.4, 3.2 Hz, 3H), 2.17 (dd, J = 6.0, 2.8 Hz, 3H). ^{13}C NMR (400 MHz, CD_2Cl_2) δ: 154.96, 149.89, 149.60, 148.04, 148.00, 147.39, 147.28, 141.20, 140.00, 138.63, 137.93, 136.27, 131.80, 130.63, 130.06, 139.87, 129.82, 129.71, 129.39, 129.18, 128.90, 125.86, 125.65, 124.80, 124.50, 124.33, 124.31, 123.46, 122.44, 122.09, 121.11, 116.96, 15.94, 14.07.

2.6 Synthetic of 2TPA

A mixture of **2** (150 mg, 0.475 mmol) and 4-(diphenylamino)benzaldehyde (285 mg, 1.04 mmol) was dissolved in toluene, which was heated at 120 °C using acetic acid (0.04 mL) and piperidine (0.04 mL) as a catalyst. Then the mixture was poured into brine, extracted with CH_2Cl_2 three times (60 mL), then washed with brine and dried with anhydrous sodium sulfate. The solvent was removed by rotary evaporation, and the crude product was purified by column chromatography (silica gel, DCM : PE = 1 : 3.5, v/v) to afford compound **2TPA** (94.2 mg, 24% yield). ^{1}H NMR (400 MHz, CD_2Cl_2) δ: 7.56 (d, J = 15.4 Hz, 2H), 7.48 (d, J = 8.2 Hz, 4H), 7.37

– 7.26 (m, 10H), 7.12 (dd, *J* = 14.4, 7.4 Hz, 12H), 7.00 (d, *J* = 8.6 Hz, 4H), 6.84 (s, 2H), 2.36 (d, *J* = 3.0 Hz, 6H).

3. Spectroscopic study

3.1 Fluorescence quantum yield

The fluorescence quantum yield (QY) was determined according to following equation:

$$\phi_{sample} = \phi_{MB} \times \frac{I^{sample}\, A^{MB}}{I^{MB}\, A^{sample}} \times [\frac{\eta^{sample}}{\eta^{MB}}]^2$$

Where ϕ_{MB} was the QY of reference, I was the area under the emission spectra, A was the absorbance at the excitation wavelength, and η was the refractive index of the used solvent. "Sample" and "MB" stand for compounds and reference, respectively. The fluorescence quantum yield was determined by measuring emission spectrum with MB in EtOH (Φ_F = 13.2%) as a reference, and the absorbance at the respective excitation wavelengths was controlled to be lower than 0.05.

3.2 Laser power density

The laser power density was determined according to following equation:

$$Laser\ power\ density\left(\frac{mW}{cm^2}\right) = \frac{Outpower\ (mW)}{Area\ of\ the\ spot\ (cm^2)}$$

Where the "Output power" could be read from the 660 nm laser, and the "Area of the spot" was the beam area which could be calculated based on the equation $\pi \times \frac{D^2}{4}$ (D is beam diameter).

3.3 Singlet oxygen ($^1O_2$) production

The singlet oxygen quantum yield (Φ_Δ) was determined according to following equation:

$$\phi_\Delta(^1O_2)^{sample} = \phi_\Delta(^1O_2)^{MB} \times \frac{S^{sample}\, F^{MB}}{S^{MB}\, F^{sample}}$$

Where "sample" and "MB" stand for the compounds and the reference, respectively. S was the slope of the change in absorbance of DPBF at the absorbance maxima with the irradiation time (808 nm, 0.1 W/cm^2). F is the absorption correction factor, which is given as $F = 1 - 10^{-OD}$.

3.4 Photophysical properties

UV-vis-NIR absorption spectra were measured at room temperature on a Shimadzu UV-3600 spectrophotometer or perkinElmer Lambda 35 with a resolution of 1.0 nm, using quartz cuvettes of 1 cm path length.

NIR-I emission spectra of **3TPA** and **2TPA** were measured on a FLUOROMAX-4 spectrometer under air atmosphere at room temperature; NIR-II emission spectra of **3TPA** and **2TPA** were recorded on 3-D Fluorescence Spectrometer.

4. Nanoparticles Preparation

A mixture of photothermal agents (1.1 mg for **3TPA** or 1.0 mg for **2TPA**) and DSPE-mPEG$_{5K}$ (10-15 mg) were dissolved in $CHCl_3$ (5 mL). The mixture was stirred at room

temperature for 2 h and dried over under vacuum to remove $CHCl_3$. Then, 10 mL of PBS was added in to the obtained lipidic film, and the solution was kept in sonication for 50 min. After passing through a 0.2 μm syringe filter, the nanoparticles suspension was obtained and stored at 4℃ for further use.

5. Photothermal effect and PCE calculation

For the purpose of evaluating the photothermal ability of **3TPA NPs** and **2TPA NPs**, first, we discussed the effect of power density on conversion efficiency. **3TPA NPs** or **2TPA NPs** were irradiated by 808 nm laser at different power densities (0.1 W/cm^2, 0.2 W/cm^2, 0.3 W/cm^2 , 0.4 W/cm^2, 0.5 W/cm^2, 0.6 W/cm^2). The temperature changes were monitored by FLIR-E40 thermal camera. Next, we considered the effect of concentration on temperature. Different concentrations of **3TPA NPs** or **2TPA NPs** were prepared (6.25 μM, 12.5 μM, 25 μM, 50 μM and 100 μM), and irradiated by 0.5 W/cm^2 with 808 nm laser for 10 min. The temperature changes were monitored during irradiation.

$$\eta = \frac{hA(T_{Max} - T_{Surr}) - Q_{Dis}}{I(1 - 10^{-A})}$$

where h represents the heat transfer coefficient, A is the surface area of the container, I is the incident laser power, A is the absorbance of the sample.

6. Cell experiment

6.1 Cell incubation

MCF-7 cells and 4T1 cells were cultured in RPMI-1640 culture medium supplemented with 10% fetal bovine serum (FBS; Gibco) and glutamine (2 mM) in an atmosphere of 5% CO_2 and 95% air at 37°C. The cells were maintained in an exponential growth phase by periodic subcultivation. The cell density was determined using a hemocytometer, and this was performed prior to any experiments.

6.2 Cytotoxicity test

The cytotoxicity of **3TPA NPs** was tested by the MTT assay on MCF-7 cells via the cleavage of MTT to purple formazan crystals by mitochondrial dehydrogenases. MCF-7 cells were plated (4.5×10^4 cells/well) in a 96-well plate at 37℃ in a humidified atmosphere with 5% CO_2 for 24 h. MCF-7 cells were then incubated with different concentrations of **3TPA NPs** or **2TPA NPs** at 37℃ in incubator. Then the plate was irradiated with or without 808 nm light at 0.75 W/cm^2 optical density and then incubated in for 24 h. Media was replaced with 2.5 mg/mL MTT reagent in PBS, and incubated for 4 h at 37℃. Cells were then dissolved using 150 μL DMSO. The absorbance at 570 nm was determined using a Varioskan Flash microplate reader.

6.3 Live/dead cells assay

MCF-7 cells were seeded at confocal culture dishes and pre-incubated for 24 h. Then, 10 μM concentration of **2TPA NPs** or **3TPA NPs** were added and incubated for 6 h, then the cells were washed with PBS for 3 times and irradiation with 0.75 W/cm^2 808 nm laser for 10 mins. Then, the culture dishes were scanned under confocal microscopy at 488 nm excitation, 500-550 nm was collected for Calcein AM and 600-650 nm was collected for PI.

6.4 Flow cytometry experiments

Annexin V-FITC/PI Apoptosis Detection Kit was used for detection of **2TPA NPs** or **3TPA NPs** mediated induced cell Apoptosis. MCF-7 cells were seeded into 6-well plates for 24 h. Then, 10 μM concentration of **2TPA NPs** or **3TPA NPs** were added and incubated for 6 h, and cells were followed by 0.8 W/cm^2 808 nm laser. After incubation for 18 h, cells were stained with Annexin V-FITC/PI Apoptosis Detection Kit according to the manufacture instruction, and analyzed using a BD LSR Fortessa flow cytometry. At least 10000 events were acquired for each sample.

7.Animal experiment

All of MCF-7 xenograft tumor-bearing BALB/c mice were anesthetized by inhalation of isoflurane before injection and during imaging. Overall procedures were approved by the Animal Ethics Committee in S10 Nanjing University (SCXK(Su)-2018-0008).

7.1 In vivo fluorescence imaging of mice

7.1.1 NIR-I fluorescence imaging

To evaluate the NIR-I fluorescence imaging performance, we used an IVIS Lumina K Series III instrument (PerkinElmer) using excitation at 760 nm and collect band path of 845 ± 20 nm. The 4T1 tumor-bearing mice were intravenously injected with 200 μL **2TPA NPs** or **3TPA NPs** solution (100 μM), and fluorescence imaging was taken 0~144 h post intratumor injection.

7.1.2 NIR-II fluorescence imaging

To evaluate the NIR-II fluorescence imaging performance, we used excitation at 808 nm and collect wavelengths in the band after 1000 nm. The 4T1 tumor-bearing mice were intravenously injected with 200 μL **2TPA NPs** or **3TPA NPs** solution (100 μM), and fluorescence imaging was taken 0~144 h post intratumor injection.

7.2 Photothermal imaging

Thermal imaging was performed with the American FLIR infrared thermal imaging equipment. PBS, **2TPA NPs** or **3TPA NPs** solution (100 μM, 200 μL) was injected into the tumor-bearing mice. After 12 h, the power density of 808 nm laser was 0.6 W/cm^2 or 0.8 W/cm^2 to illuminate the tumor area and record the temperature of the tumor area.

7.2 In vivo PTT

Five-week-old female BALB/c mice were purchased from the Model Animal Research Center of Nanjing University (MARC). To establish the xenograft 4T1 tumor-bearing mouse model, murine 4T1 breast cancer cells (5×10^5) suspended in 100 μL of RPMI-1640 medium were injected subcutaneously into the right back of the mouse.

After about 10 days, mice with tumor volumes at about 50-80 mm^3 were used subsequently. The 4T1-tumor-bearing mice were randomly divided into 5 groups (PBS, **2TPA NPs** + Dark, **2TPA NPs** + Light, **3TPA NPs** + Dark, **3TPA NPs** + Light, N=5 independent groups mice). 150 μL 100 μM solution were injected into the tumor-bearing mice through tail vein using a

microsyringe. After 12 h, the power density of 808 nm laser was 0.75 W/cm^2 and the exposure time was 10 mins. During therapy, the tumor volumes and body weights were measured every two days. The mice were euthanized under enflurane gas anesthesia till 14 days posttreatment according to institutional guidelines, tumors were resected and weighed.

7.3 H&E staining

After 14 days of various treatments, the above-mentioned 5 groups of mice were sacrificed. The heart, liver, spleen, lung, kidney and tumor were excised, fixed in 4% formalin solution, and sectioned at 5 μm thickness. After conventional H&E staining, the slices were examined with a digital microscope (Leica QWin).

8. Results and Discussion

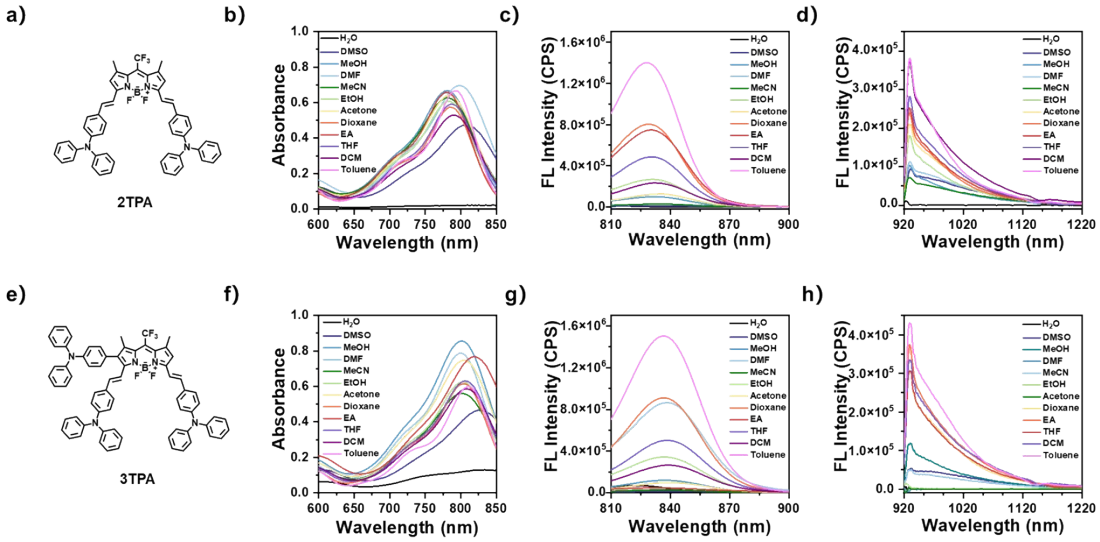

Figure S1. Photophysical properties of **2TPA** and **3TPA** in different solvents. (a) Chemical structures, (b) Absorption spectra, (c) Fluorescence spectra (λ_{ex} = 764 nm) and (d) Fluorescence spectra of **2TPA** (5 μM) in different solvents (λ_{ex} = 823 nm); (e) Chemical structures, (f) Absorption spectra, (g) Fluorescence spectra (λ_{ex} = 767 nm) and (h) Fluorescence spectra of **3TPA** (5 μM) in different solvents (λ_{ex} = 825 nm).

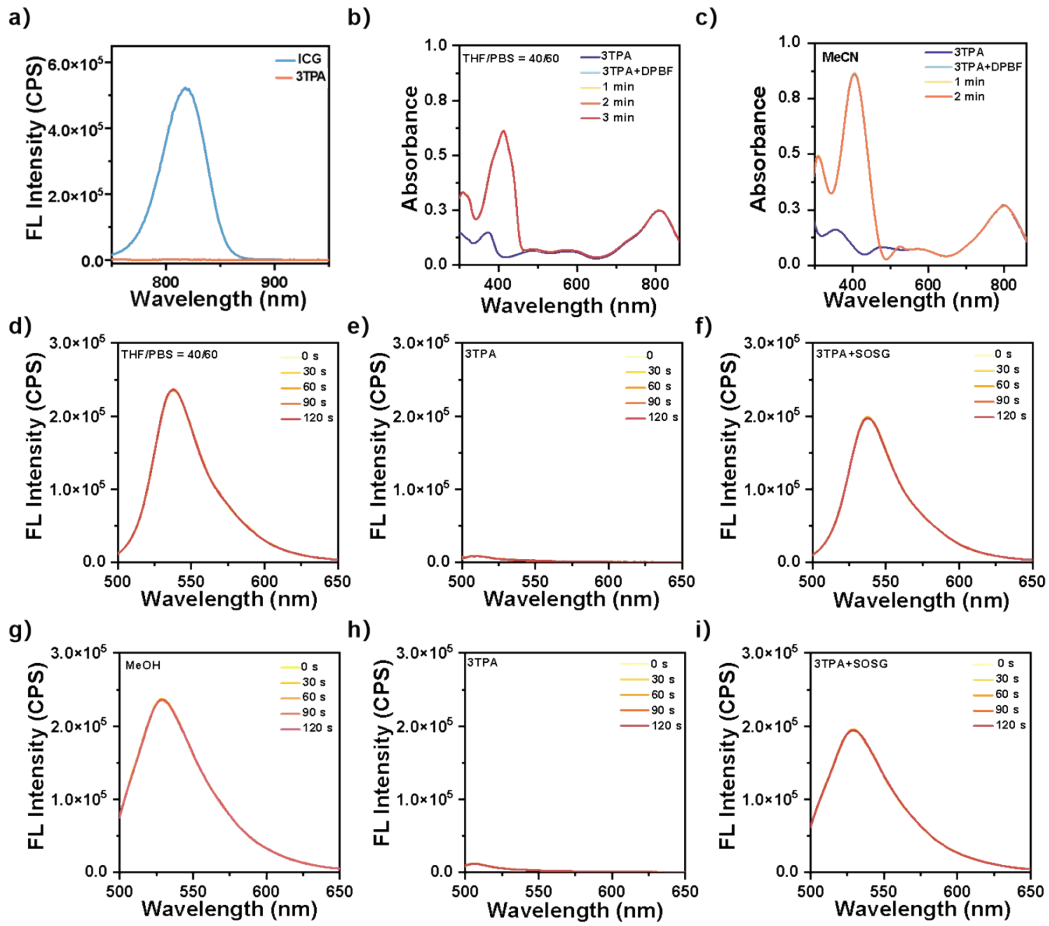

Figure S2. (a) Fluorescence spectra of **3TPA** (5 μM) in DCM. The fluorescence quantum yields were determined using ICG (Φ_f = 13.2% (EtOH)) for **3TPA** as reference (λ_{ex} = 720 nm). Changes of absorption spectra of DPBF in the presence of **3TPA** in THF and PBS mixed solvent (b) and MeCN (c) under different durations of light irradiation (0.1 W/cm^2). Fluorescence enhancement of the 5 μM SOSG in the presence of the $^1O_2$ produced by 5 μM 3TPA in THF and PBS mixed solvent (d-f)and MeOH (g-i) upon 808 nm laser irradiation (0.1 W/cm^2).

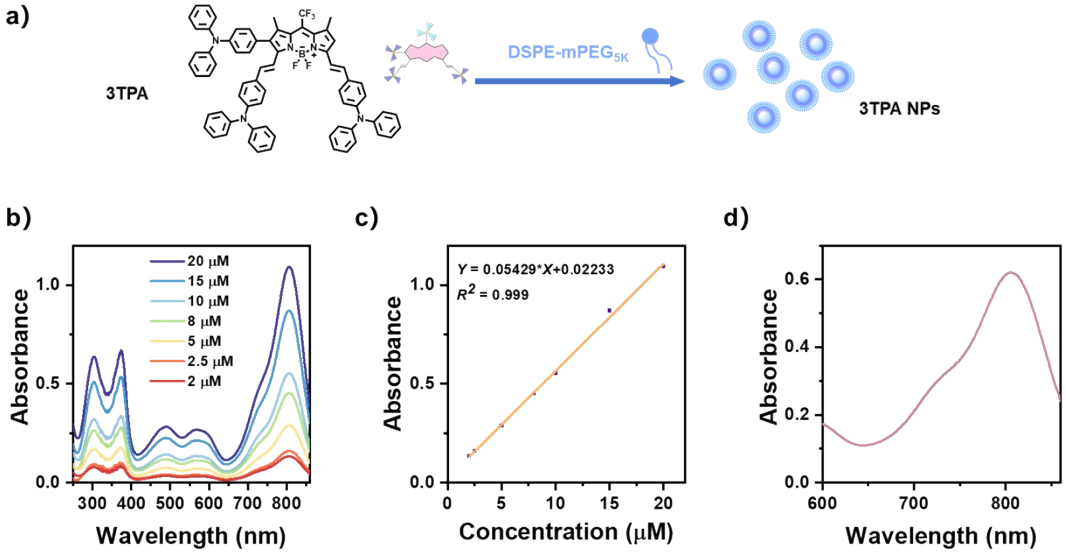

Figure S3. Determination of the loading efficiency of **3TPA NPs**. (a) Preparation of **3TPA NPs**. (b) UV-Vis spectra of **3TPA** dissolved in THF at different concentrations. (c) Fitted calibration curve of UV-Vis absorbance vs. concentration of **3TPA** in THF at 807 nm. (d) UV-Vis spectrum of as-prepared **3TPA NPs** dissolved in THF (diluted 150 times). The concentration of **3TPA** in the **3TPA NPs** solution was calculated to be 0.0110 mM, thus the loading efficiency of **3TPA** in NPs was about 91% (0.0110 mM·150 / 1.75 mM·100% = 94.4%).

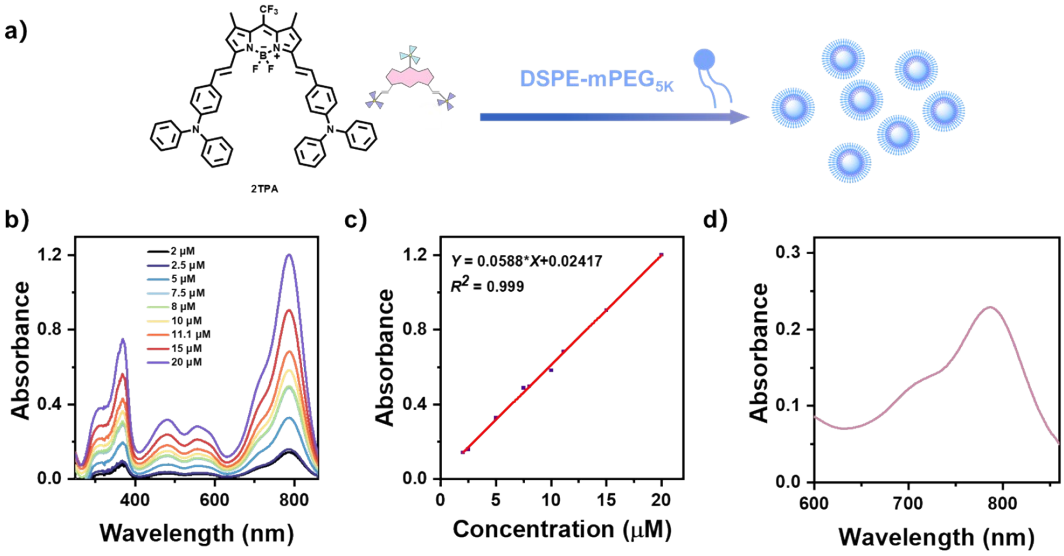

Figure S4. Preparation and Characterization of Nanoparticles. (a) Preparation of **2TPA NPs**. (b) UV-Vis spectra of **2TPA** dissolved in THF at different concentrations. (c) Fitted calibration curve of UV-Vis absorbance vs. concentration of **2TPA** in THF at 785 nm. (d) UV-Vis spectrum of as-prepared **2TPA NPs** dissolved in THF (diluted 150 times). The concentration of **2TPA** in the **2TPA NPs** solution was calculated to be 3.47 μM, thus the loading efficiency of **3TPA** in NPs was about 91% (3.47 μM·150 / 555 μM·100% = 93.7%).

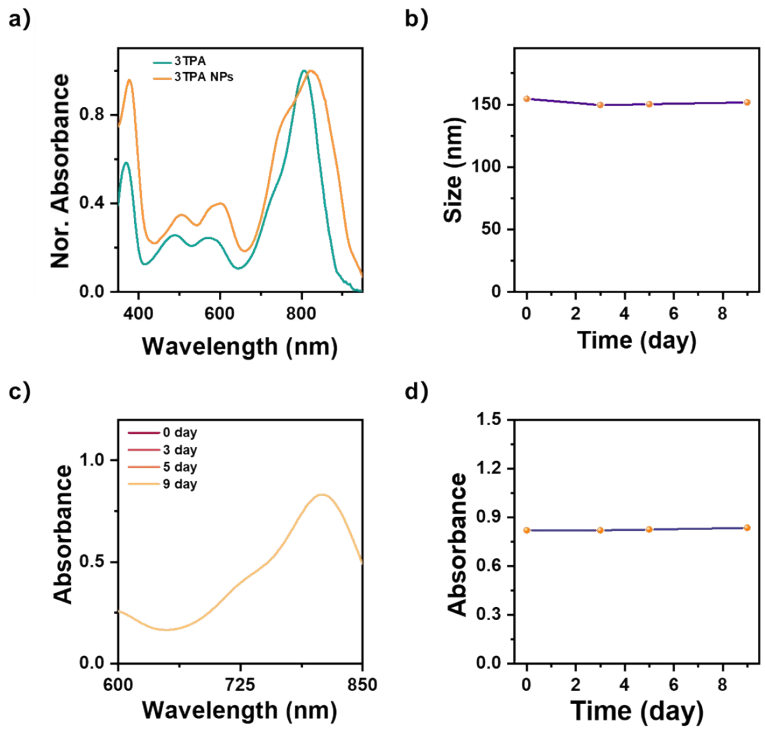

Figure S5. (a) Normalized absorption spectra of **3TPA** and **3TPA NPs** in PBS buffer (pH = 7.4); Average diameter (b) and absorbance (c-d) of **3TPA NPs** store for different time measured by DLS and UV-Vis spectrum.

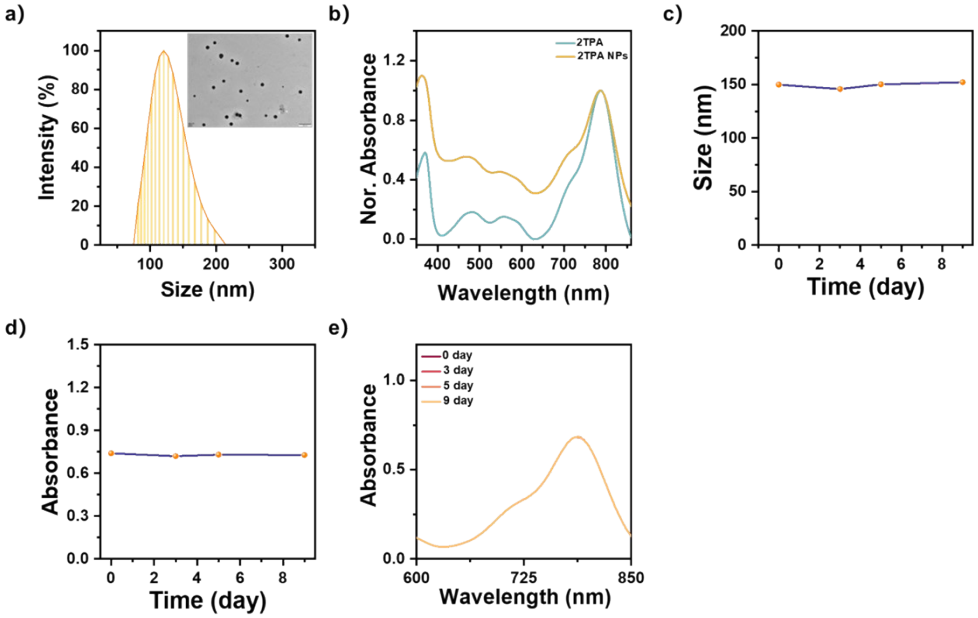

Figure S6. Characterization of Nanoparticles. (a) Particle size distribution of **2TPA NPs** measured by DLS with a mean diameter of 140 nm and a PDI of 0.17, Inset: TEM image (top right) of **2TPA NPs**; (b) Normalized absorption spectra of **2TPA** and **2TPA NPs** in PBS buffer (pH = 7.4); Average diameter (c) and absorbance (d-e) of **2TPA NPs** store for different time measured by DLS and UV-Vis spectrum.

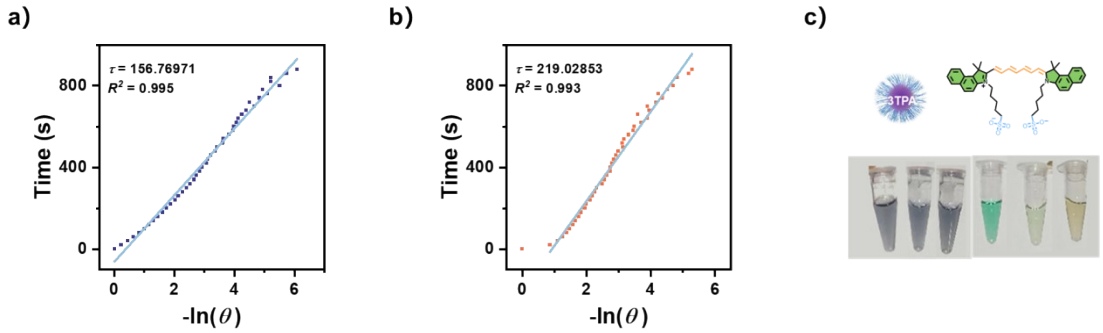

Figure S7. Time constants for calculating photothermal conversion efficiency of (a) **3TPA NPs** and (b) ICG; (c) Solution color changes of **3TPA NPs** and ICG after 1st, 3rd, and 6th hot and cold cycles.

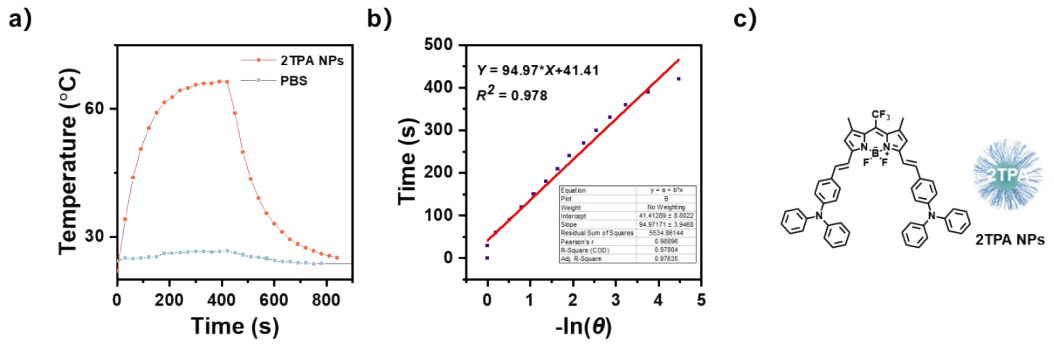

Figure S8. Photothermal properties of **2TPA NPs** in PBS buffer (pH = 7.4). (a) Photothermic heating curves of **2TPA NPs** (50 μM) dispersions under 808 nm irradiation (0.75 W/cm^2) with 150 μL followed by cooling to room temperature; (b) Infrared imaging of **2TPA NPs** dispersions; (c) Chemical structure of **2TPA NPs**.

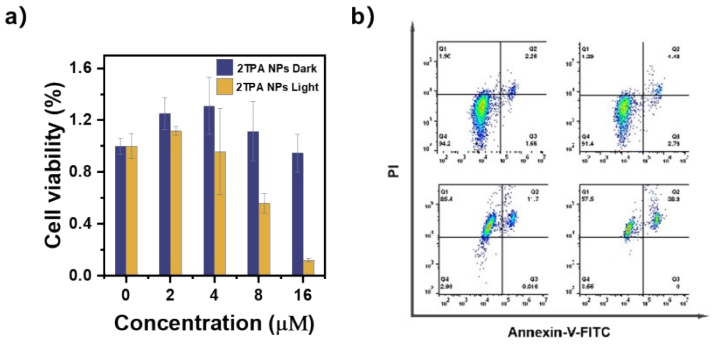

Figure S9. Cytotoxicity assessment of **2TPA NPs**. (a) Cell viability of MCF-7 cells incubated with **2TPA NPs** at various concentrations in the dark and after laser irradiation (808 nm, 0.75 W/cm^2, 10 min); (b) Apoptosis and necrosis analysis using flow cytometry toward MCF-7 cells after different treatments. Laser irradiation (808 nm, 0.5 W/cm^2, 10 min) was conducted after cells were incubated with **2TPA NPs** (10 μM).

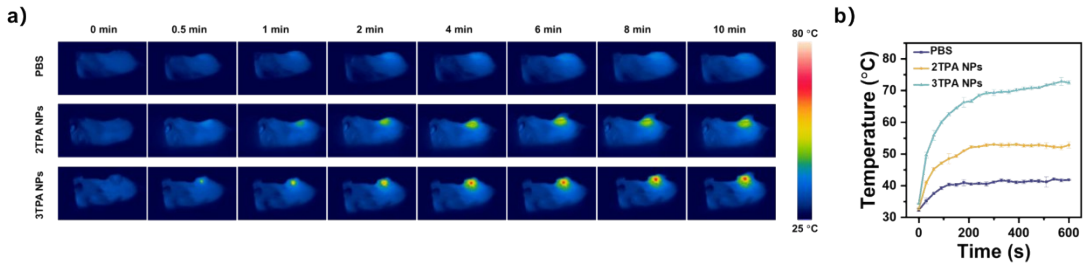

Figure S10. Infrared thermal imaging of 4T1 tumor-bearing mice. (a) Infrared thermal imaging of 4T1 tumor-bearing mice treated with PBS, **2TPA NPs** and **3TPA NPs** exposed to 808 nm laser (0.8 W/cm^2) recorded at different time intervals, respectively; (b) Temperature profiles of tumor-site as a function of irradiation time.

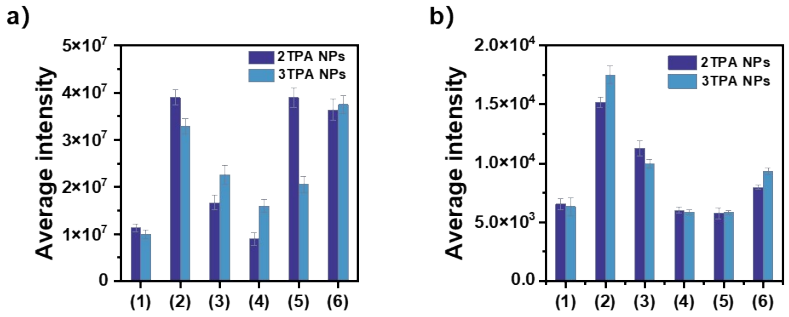

Figure S11. NIR-I (a) and NIR-II (b) fluorescence intensity profiles of **2TPA NPs** and **3TPA NPs** in the different organ regions and tumor regions including (1) Heart, (2) Liver, (3) Spleen, (4) Lung, (5) Kidney and (6) tumor.

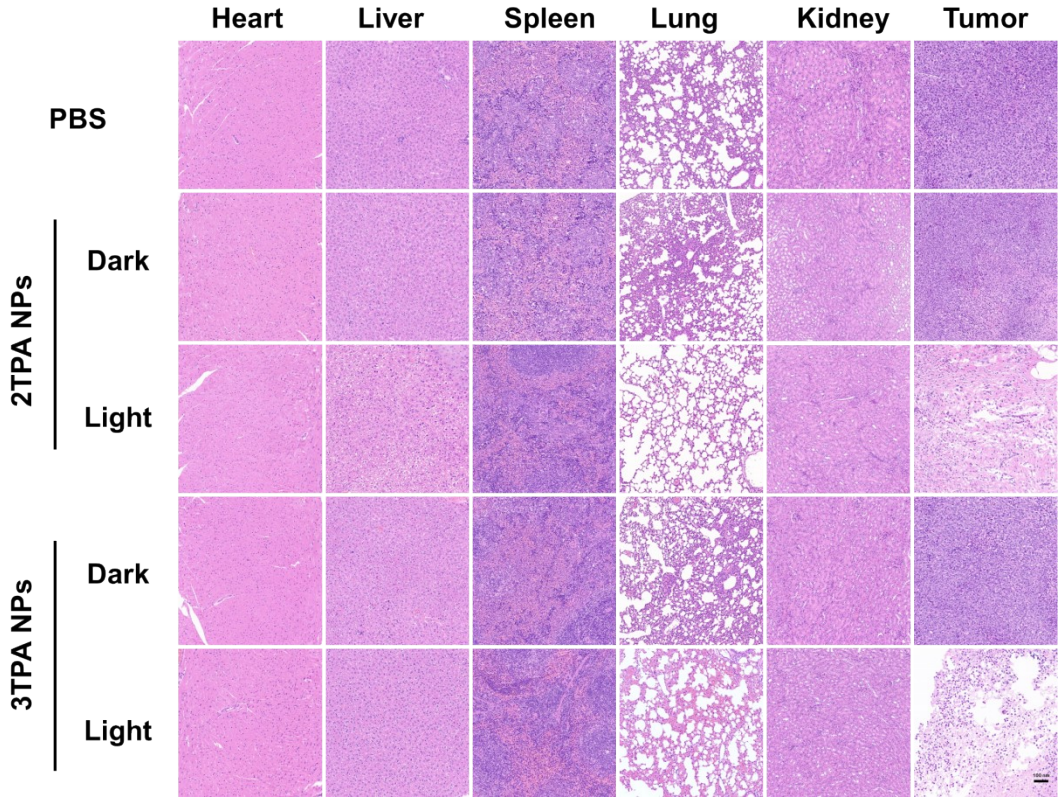

Figure S12. H&E staining analysis of tumor tissue sections from three groups of mice. All the images shared the same scale bar of 100 μm.

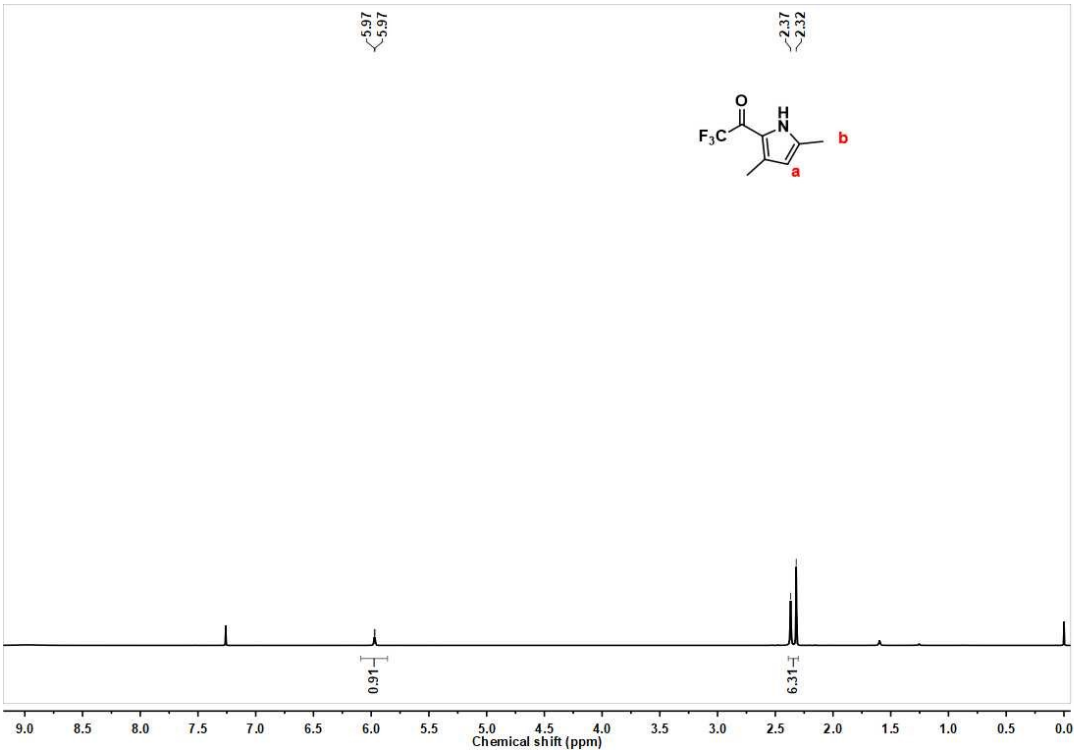

Figure S13. ^{1}H NMR of **1** in $CDCl_3$ (400 Hz)

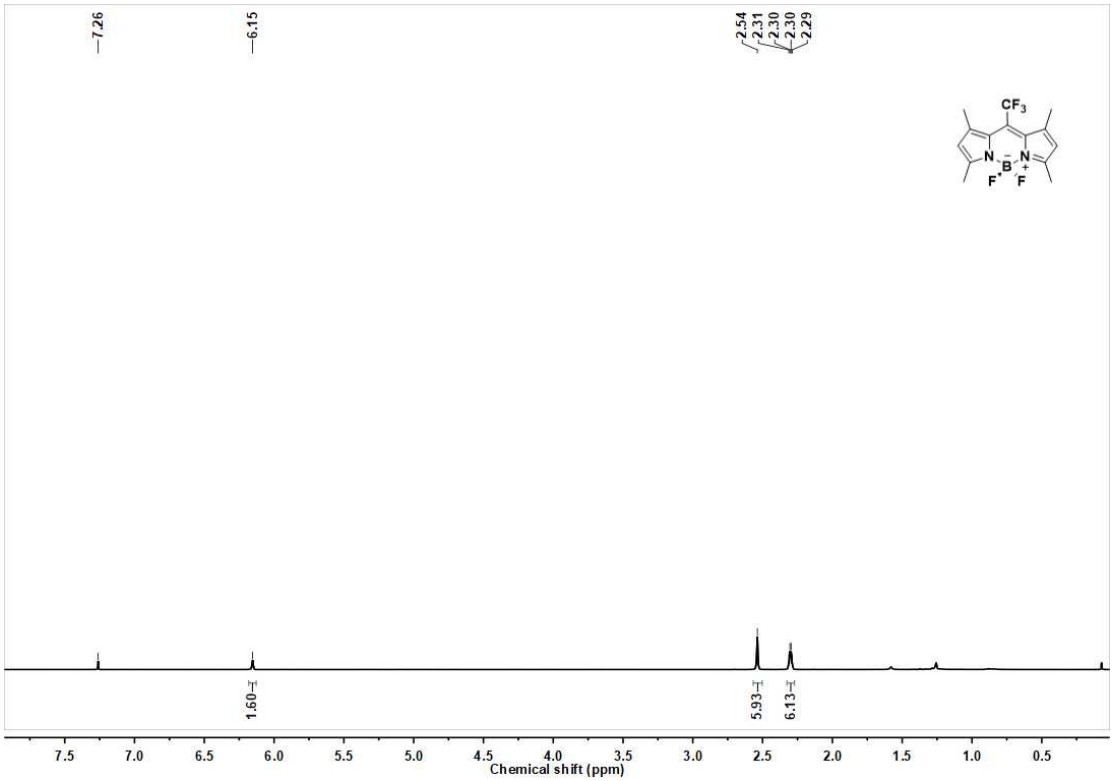

Figure S14. ^{1}H NMR of **2** in $CDCl_3$ (400 Hz)

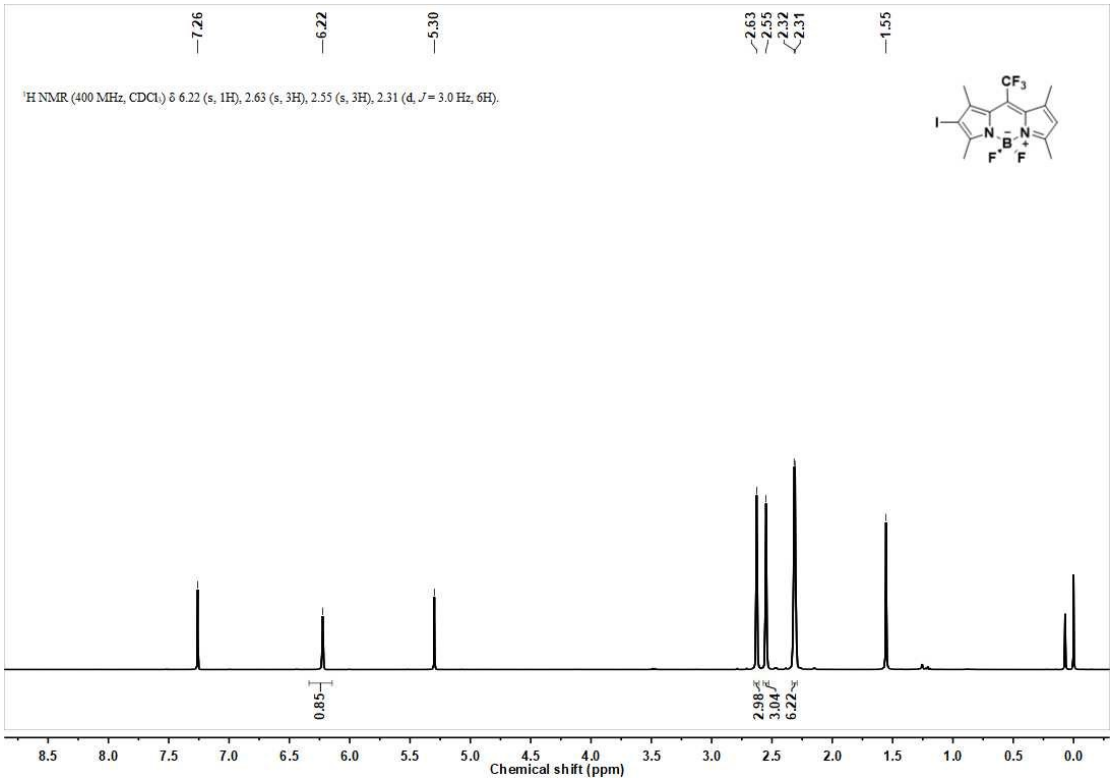

Figure S15. ^{1}H NMR of **3** in $CDCl_3$ (400 Hz)

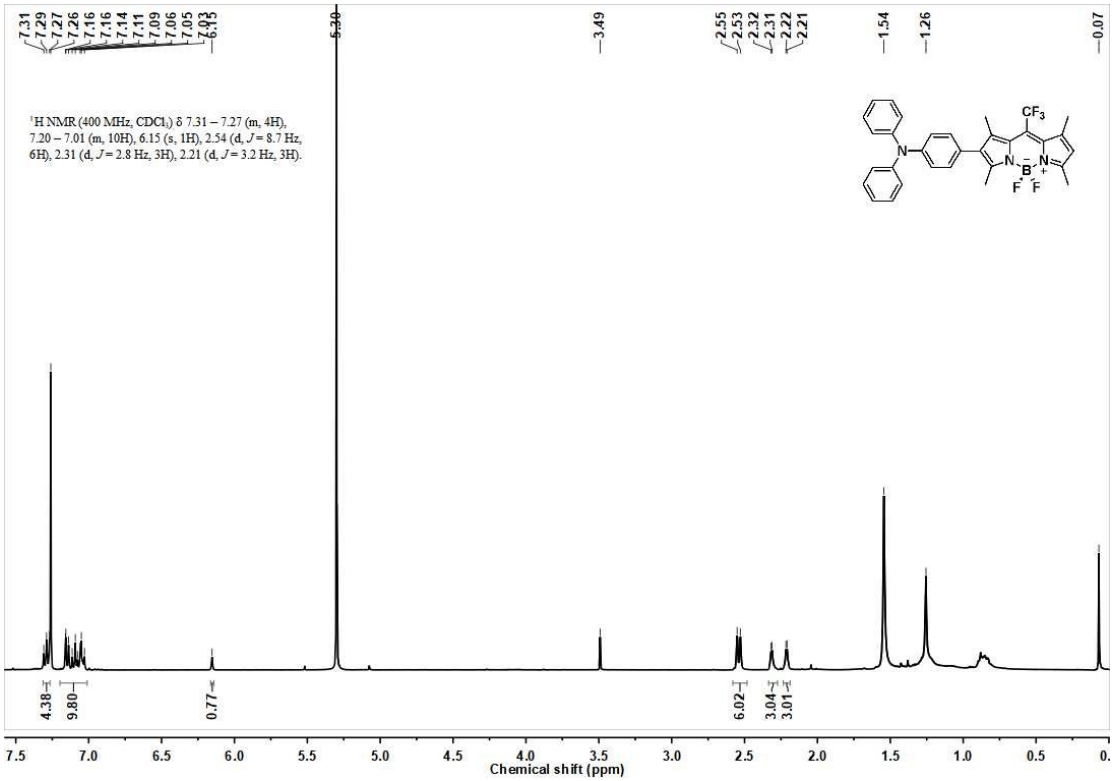

Figure S16. ^{1}H NMR of **4** in $CDCl_3$ (400 Hz)

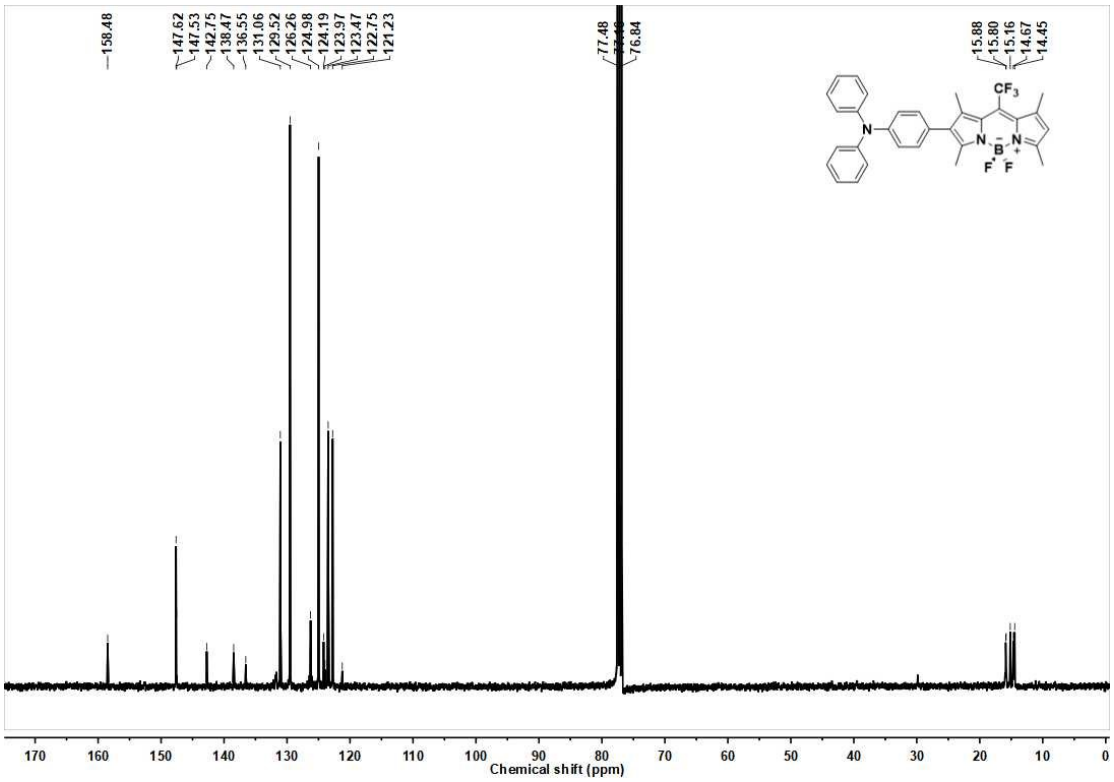

Figure S17. ^{13}C NMR of **4** in $CDCl_3$ (400 Hz)

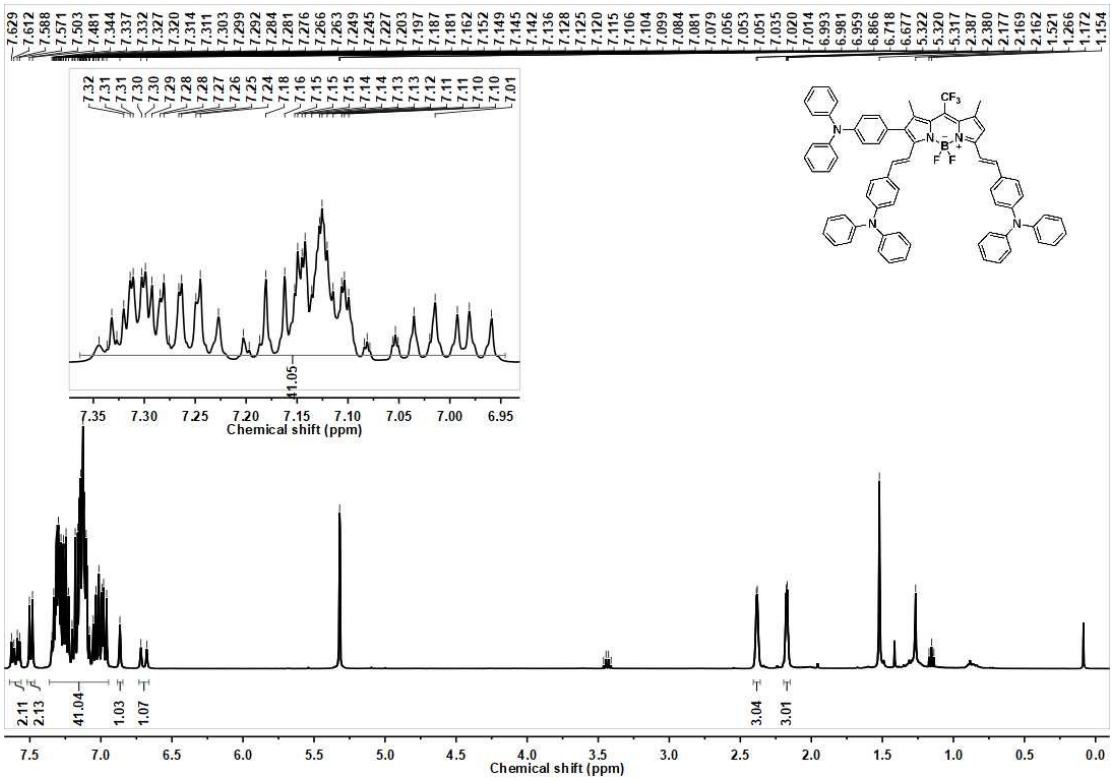

Figure S18. ^{1}H NMR of **3TPA** in $CDCl_3$ (400 Hz)

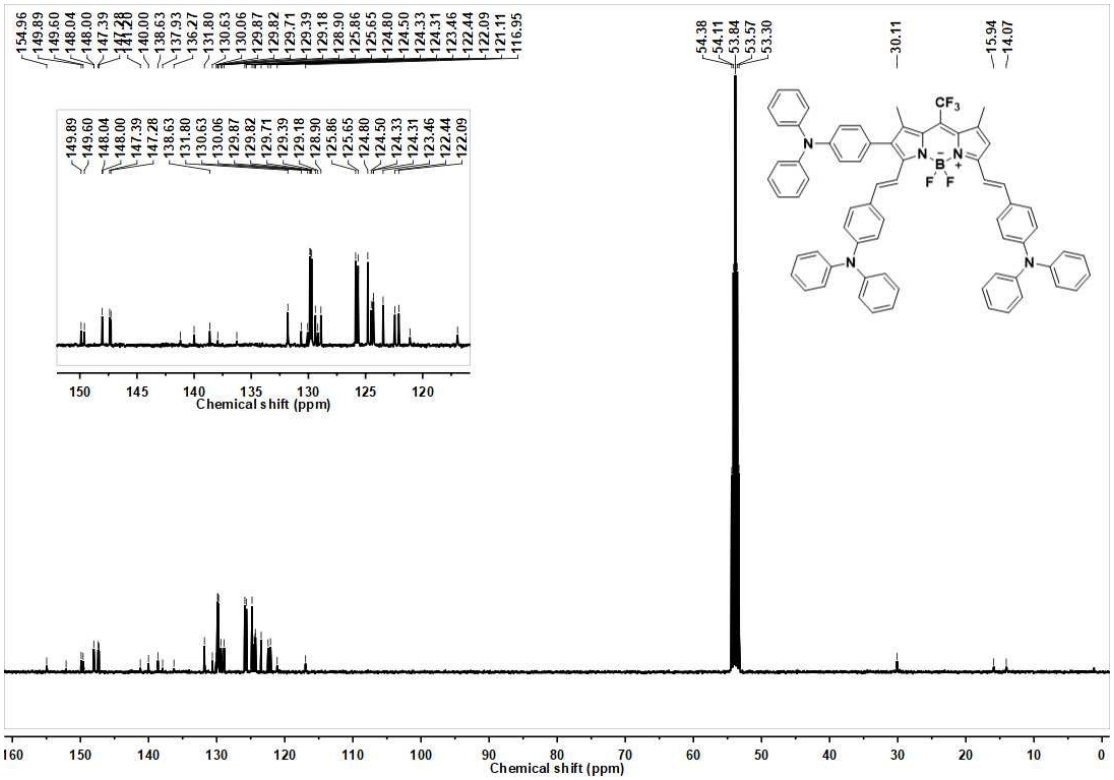

Figure S19. ^{13}C NMR of **3TPA** in $CDCl_3$ (400 Hz)

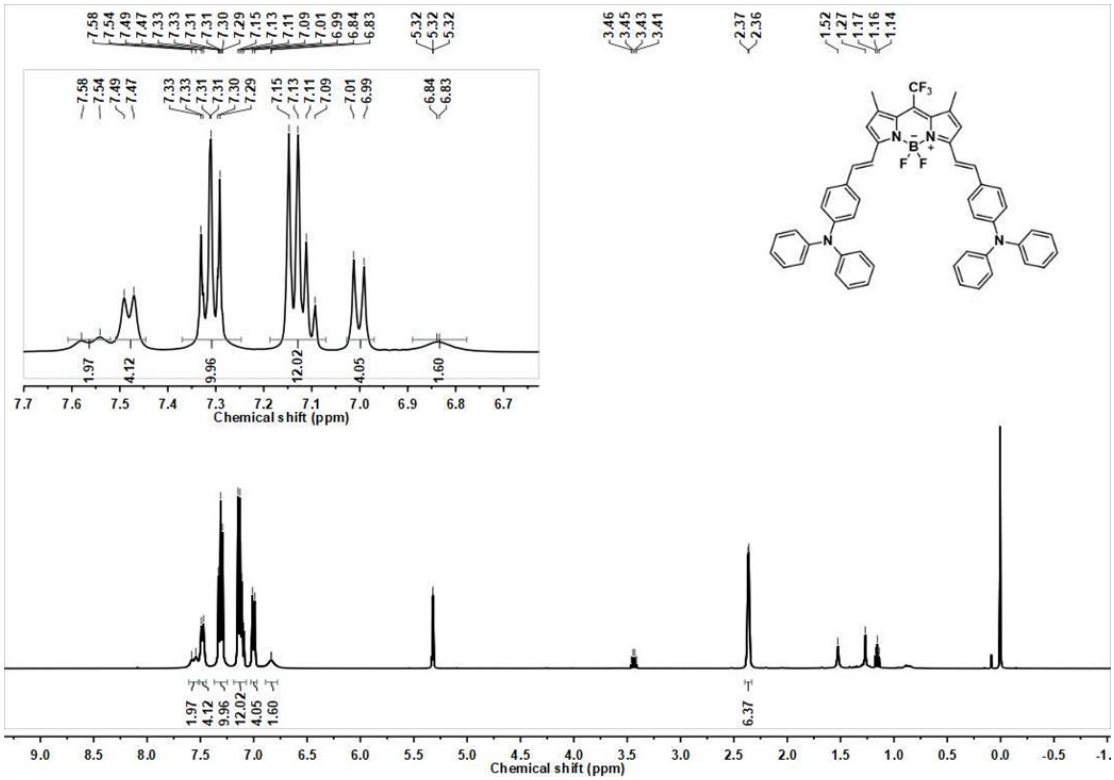

Figure S20. ^{1}H NMR of **2TPA** in $CDCl_3$ (400 Hz)